Please cite this article in press as: Ran et al., Double Nicking by RNA-Guided CRISPR Cas9 for Enhanced Genome Editing Specificity, Cell (2013), http://dx.doi.org/10.1016/j.cell.2013.08.021

Resource

Cell

Double Nicking by RNA-Guided CRISPR Cas9 for Enhanced Genome Editing Specificity

F. Ann Ran,[1,2,3,4,5,11] Patrick D. Hsu,[1,2,3,4,5,11] Chie-Yu Lin,[1,2,3,4,6] Jonathan S. Gootenberg,[1,2,3,4] Silvana Konermann,[1,2,3,4] Alexandro E. Trevino,[1] David A. Scott,[1,2,3,4] Azusa Inoue,[7,8,9,10] Shogo Matoba,[7,8,9,10] Yi Zhang,[7,8,9,10] and Feng Zhang[1,2,3,4,*]

[1]Broad Institute of MIT and Harvard, 7 Cambridge Center, Cambridge, MA 02142, USA
[2]McGovern Institute for Brain Research
[3]Department of Brain and Cognitive Sciences
[4]Department of Biological Engineering
Massachusetts Institute of Technology, Cambridge, MA 02139, USA
[5]Department of Molecular and Cellular Biology, Harvard University, Cambridge, MA 02138, USA
[6]Harvard/MIT Division of Health Sciences and Technology
[7]Howard Hughes Medical Institute
[8]Program in Cellular and Molecular Medicine
[9]Department of Genetics
[10]Harvard Stem Cell Institute
Harvard Medical School, Boston, MA 02115, USA
[11]These authors contributed equally to this work
*Correspondence: zhang@broadinstitute.org
http://dx.doi.org/10.1016/j.cell.2013.08.021

SUMMARY

Targeted genome editing technologies have enabled a broad range of research and medical applications. The Cas9 nuclease from the microbial CRISPR-Cas system is targeted to specific genomic loci by a 20 nt guide sequence, which can tolerate certain mismatches to the DNA target and thereby promote undesired off-target mutagenesis. Here, we describe an approach that combines a Cas9 nickase mutant with paired guide RNAs to introduce targeted double-strand breaks. Because individual nicks in the genome are repaired with high fidelity, simultaneous nicking via appropriately offset guide RNAs is required for double-stranded breaks and extends the number of specifically recognized bases for target cleavage. We demonstrate that using paired nicking can reduce off-target activity by 50- to 1,500-fold in cell lines and to facilitate gene knockout in mouse zygotes without sacrificing on-target cleavage efficiency. This versatile strategy enables a wide variety of genome editing applications that require high specificity.

INTRODUCTION

The ability to perturb the genome in a precise and targeted fashion is crucial for understanding genetic contributions to biology and disease. Genome engineering of cell lines or animal models has traditionally been accomplished through random mutagenesis or low-efficiency gene targeting. To facilitate genome editing, programmable sequence-specific DNA nuclease technologies have enabled targeted modification of endogenous genomic sequences with high efficiency, particularly in species that have proven traditionally genetically intractable (Carlson et al., 2012; Geurts et al., 2009; Takasu et al., 2010; Watanabe et al., 2012). The RNA-guided Cas9 nucleases from the microbial CRISPR (clustered regularly interspaced short palindromic repeat)-Cas systems are robust and versatile tools for stimulating targeted double-stranded DNA breaks (DSBs) in eukaryotic cells (Chang et al., 2013; Cho et al., 2013; Cong et al., 2013; Deltcheva et al., 2011; Deveau et al., 2010; Friedland et al., 2013; Gratz et al., 2013; Horvath and Barrangou, 2010; Jinek et al., 2013; Mali et al., 2013b; Wang et al., 2013), where the resulting cellular repair mechanisms—nonhomologous end-joining (NHEJ) or homology-directed repair (HDR) pathways—can be exploited to induce error-prone or defined alterations (Hsu and Zhang, 2012; Perez et al., 2008; Urnov et al., 2010).

The Cas9 nuclease from *Streptococcus pyogenes* can be directed by a chimeric single-guide RNA (sgRNA) (Jinek et al., 2012) to any genomic locus followed by a 5′-NGG protospacer-adjacent motif (PAM). A 20 nt guide sequence within the sgRNA directs Cas9 to the genomic target via Watson-Crick base pairing and can be easily programmed to target a desired genomic locus (Deltcheva et al., 2011; Deveau et al., 2010; Gasiunas et al., 2012; Jinek et al., 2012). Recent studies of Cas9 specificity have demonstrated that, although each base within the 20 nt guide sequence contributes to overall specificity, multiple mismatches between the guide RNA and its complementary target DNA sequence can be tolerated depending on the quantity, position, and base identity of mismatches (Cong et al., 2013; Fu et al., 2013; Hsu et al., 2013; Jiang et al., 2013), leading to potential off-target

Please cite this article in press as: Ran et al., Double Nicking by RNA-Guided CRISPR Cas9 for Enhanced Genome Editing Specificity, Cell (2013), http://dx.doi.org/10.1016/j.cell.2013.08.021

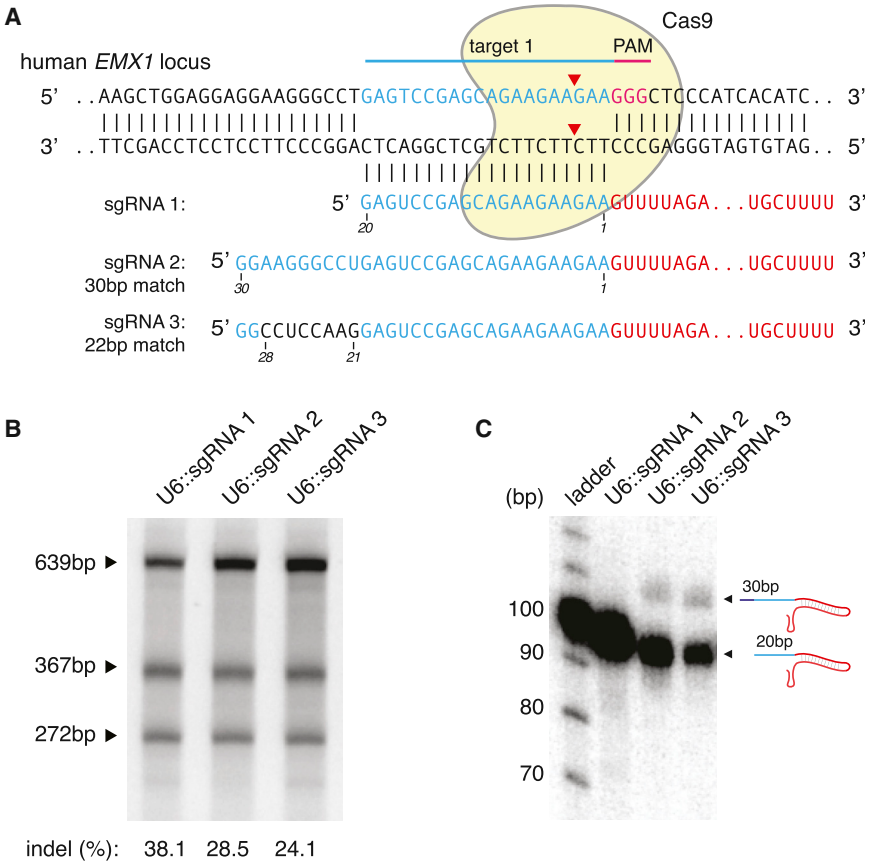

Figure 1. Effect of Guide Sequence Extension on Cas9 Activity

(A) Cas9 with matching or mismatching sgRNA sequences targeting a locus (target 1) within the human *EMX1* gene.

(B) SURVEYOR assay gel showing comparable modification of target 1 by sgRNAs bearing 20 and 30 nt long guide sequences.

(C) Northern blot showing that extended sgRNAs are largely processed to 20 nt guide-length sgRNAs in HEK293FT cells.

DSBs and indel formation. These unwanted mutations can potentially limit the utility of Cas9 for genome editing applications that require high levels of precision, such as generation of isogenic cell lines for testing causal genetic variations (Soldner et al., 2011) or in vivo and ex vivo genome-editing-based therapies.

To improve the specificity of Cas9-mediated genome editing, we developed a strategy that combines the D10A mutant nickase version of Cas9 (Cas9n) (Cong et al., 2013; Gasiunas et al., 2012; Jinek et al., 2012) with a pair of offset sgRNAs complementary to opposite strands of the target site. Whereas nicking of both DNA strands by a pair of Cas9 nickases leads to site-specific DSBs and NHEJ, individual nicks are predominantly repaired by the high-fidelity base excision repair pathway (BER) (Dianov and Hübscher, 2013). A paired nickase strategy was described while this manuscript was under review, which suggests the possibility for engineering a system to ameliorate off-target activity (Mali et al., 2013a). In a manner analogous to dimeric zinc finger nucleases (ZFNs) (Miller et al., 2007; Porteus and Baltimore, 2003; Sander et al., 2011; Wood et al., 2011) and transcription-activator-like effector nucleases (TALENs) (Boch et al., 2009; Christian et al., 2010; Miller et al., 2011; Moscou and Bogdanove, 2009; Reyon et al., 2012; Sanjana et al., 2012; Wood et al., 2011; Zhang et al., 2011), wherein DNA cleavage requires synergistic interaction of two independent specificity-encoding DNA-binding modules directing FokI nuclease monomers, this double-nicking strategy minimizes off-target mutagenesis by each individual Cas9n-sgRNA complex while maintaining on-target modification rates similar to those of wild-type Cas9. Here, we define crucial parameters for the selection of sgRNA pairs that facilitate effective double nicking, compare the specificity of wild-type Cas9 and Cas9n with double nicking, and demonstrate a variety of experimental applications that can be achieved using double nicking in cells as well as in mouse zygotes.

RESULTS

Extension of Guide Sequence Does Not Improve Cas9 Targeting Specificity

Cas9 targeting is facilitated by base pairing between the 20 nt guide sequence within the sgRNA and the target DNA (Deltcheva et al., 2011; Deveau et al., 2010; Gasiunas et al., 2012; Jinek et al., 2012). We reasoned that cleavage specificity might be improved by increasing the length of base pairing between the guide RNA and its target locus. To test this, we generated U6-driven expression cassettes (Hsu et al., 2013) to express three sgRNAs with 20 (sgRNA 1) or 30 nt guide sequences (sgRNAs 2 and 3) targeting a locus within the human *EMX1* gene (Figure 1A).

We and others have previously shown that, although single-base mismatches between the PAM-distal region of the guide sequence and target DNA are well tolerated by Cas9, multiple mismatches in this region can significantly affect on-target activity (Fu et al., 2013; Hsu et al., 2013; Mali et al., 2013a; Pattanayak et al., 2013). To determine whether additional PAM-distal bases (21–30) could influence overall targeting specificity, we designed sgRNAs 2 and 3 to contain additional bases consisting of either 10 perfectly matched or 8 mismatched bases (bases 21–28). Surprisingly, we observed that these extended sgRNAs mediated similar levels of modification at the target locus in HEK293 FT cells regardless of whether the additional bases were complementary to the genomic target (Figure 1B). Subsequent northern blots revealed that the majority of both sgRNA 2 and 3 were processed to the same length as sgRNA 1, which contains the same 20 nt guide sequence without additional bases (Figure 1C).

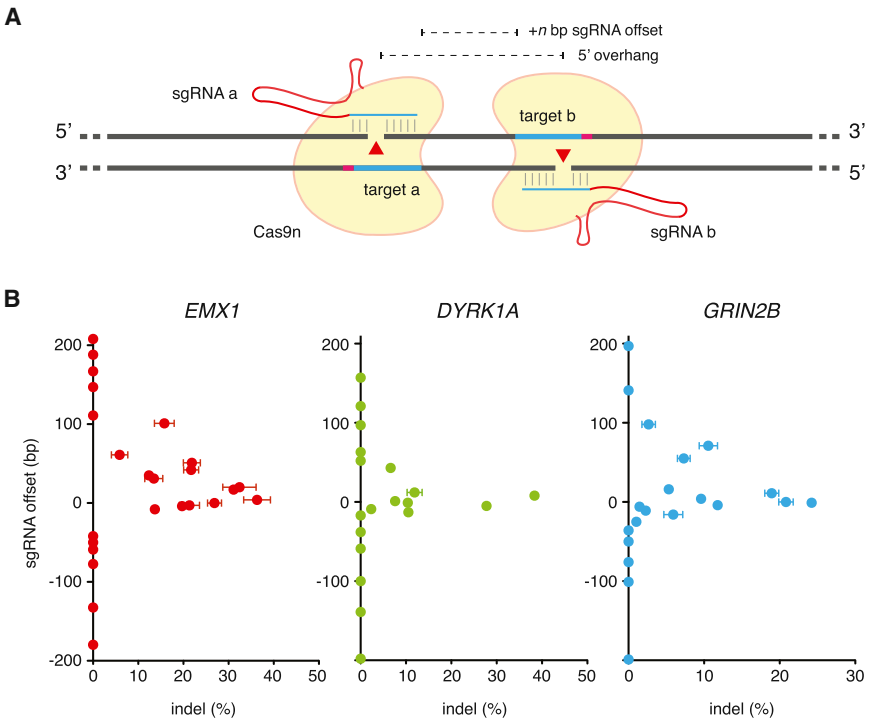

Figure 2. Double Nicking Facilitates Efficient Genome Editing in Human Cells

(A) Schematic illustrating DNA double-stranded breaks using a pair of sgRNAs guiding Cas9 D10A nickases (Cas9n). The D10A mutation renders Cas9 able to cleave only the strand complementary to the sgRNA; a pair of sgRNA-Cas9n complexes can nick both strands simultaneously. sgRNA offset is defined as the distance between the PAM-distal (5′) ends of the guide sequence of a given sgRNA pair; positive offset requires the sgRNA complementary to the top strand (sgRNA a) to be 5′ of the sgRNA complementary to the bottom strand (sgRNA b), which always creates a 5′ overhang.

(B) Efficiency of double-nicking-induced NHEJ as a function of the offset distance between two sgRNAs. Sequences for all sgRNAs used can be found in Table S1. n = 3; error bars show mean ± SEM.

(C) Representative sequences of the human *EMX1* locus targeted by Cas9n. sgRNA target sites and PAMs are indicated by blue and magenta bars, respectively. (Bottom) Selected sequences showing representative indels. See also Tables S1 and S2.

Cas9 Nickase Generates Efficient NHEJ with Paired, Offset Guide RNAs

Given that extension of the guide sequence failed to improve Cas9 targeting specificity, we sought an alternative strategy for increasing the overall base-pairing length between the guide sequence and its DNA target. Cas9 enzymes contain two conserved nuclease domains, HNH and RuvC, which cleave the DNA strand complementary and noncomplementary to the guide RNA, respectively. Mutations of the catalytic residues (D10A in RuvC and H840A in HNH) convert Cas9 into DNA nickases (Cong et al., 2013; Gasiunas et al., 2012; Jinek et al., 2012). As single-strand nicks are preferentially repaired by the high-fidelity BER pathway (Dianov and Hübscher, 2013), we reasoned that two Cas9-nicking enzymes directed by a pair of sgRNAs targeting opposite strands of a target locus could mediate DSBs while minimizing off-target activity (Figure 2A).

A number of factors may affect cooperative nicking leading to indel formation, including steric hindrance between two adjacent Cas9 molecules or Cas9-sgRNA complexes, overhang type, and sequence context; some of these may be characterized by testing multiple sgRNA pairs with distinct target sequences and offsets (the distance between the PAM-distal [5′] ends of the guide sequence of a given sgRNA pair). To systematically assess how sgRNA offsets might affect subsequent repair and generation of indels, we first designed sets of sgRNA pairs targeted against the human *EMX1* genomic locus separated by a range of offset distances from approximately −200 to 200 bp to create both 5′ and 3′ overhang products (Figure 2A and Table S1 available online). We then assessed the ability of each sgRNA pair with the D10A Cas9 mutant (referred to as Cas9n; H840A Cas9 mutant is referred to as Cas9H840A) to generate indels in human HEK 293FT cells. Robust NHEJ (up to 40%) was observed for sgRNA pairs with offsets from −4 to 20 bp, with modest indels forming in pairs offset by up to 100 bp (Figure 2B, left). We subsequently recapitulated these findings by testing similarly offset sgRNA pairs at two other genomic loci, *DYRK1A* and *GRIN2B* (Figure 2B, right). Of note, across all three loci examined, only sgRNA pairs creating 5′ overhangs with less than 8 bp overlap between the guide sequences (offset greater than −8 bp) were able to mediate detectable indel formation (Figure 2C).

Importantly, each guide used in these assays is able to efficiently induce indels when paired with wild-type Cas9 (Table S1), indicating that the relative positions of the guide pairs are the most important parameters in predicting double-nicking activity. Because Cas9n and Cas9H840A nick opposite strands of DNA, substitution of Cas9n with Cas9H840A with a given

Please cite this article in press as: Ran et al., Double Nicking by RNA-Guided CRISPR Cas9 for Enhanced Genome Editing Specificity, Cell (2013), http://dx.doi.org/10.1016/j.cell.2013.08.021

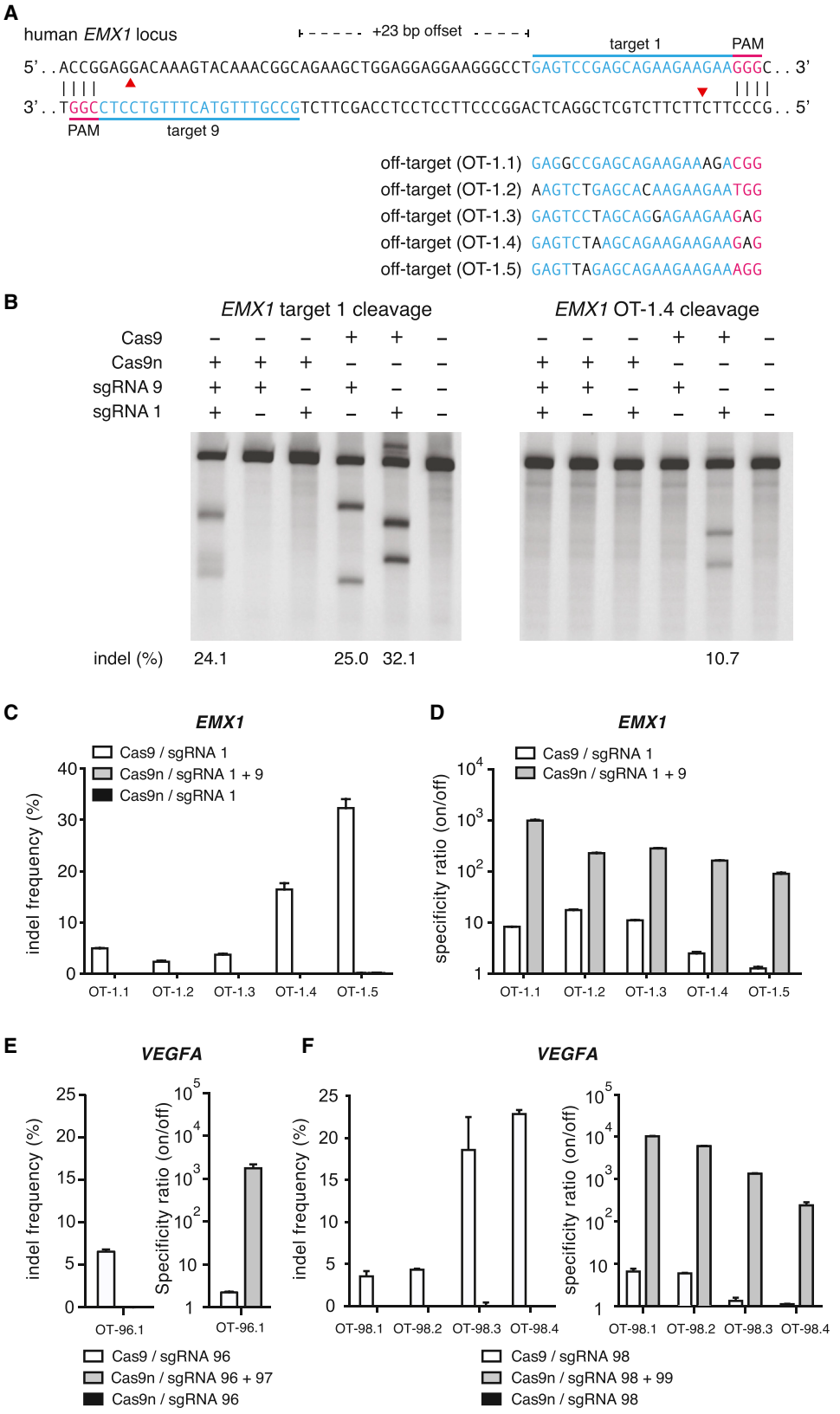

(legend on next page)

sgRNA pair should result in the inversion of the overhang type. For example, a pair of sgRNAs that will generate a 5′ overhang with Cas9n should, in principle, generate the corresponding 3′ overhang instead. Therefore, sgRNA pairs that lead to the generation of a 3′ overhang with Cas9n might be used with Cas9H840A to generate a 5′ overhang. Further work will be needed to identify the necessary design rules for sgRNA pairing to allow double nicking by Cas9H840A.

Double Nicking Mediates Efficient Genome Editing with Improved Specificity

Having established that double nicking (DN) mediates high-efficiency NHEJ at levels comparable to those induced by wild-type Cas9 (Table S1), we next studied whether DN has improved specificity over wild-type Cas9 by measuring their off-target activities. We co-delivered Cas9n with sgRNAs 1 and 9, spaced by a +23 bp offset, to target the human *EMX1* locus in HEK 293FT cells (Figure 3A). This DN configuration generated on-target indel levels similar to those generated by the wild-type Cas9 paired with each sgRNA alone (Figure 3B, left). Strikingly, unlike with wild-type Cas9, DN did not generate detectable modification at a previously validated sgRNA 1 off-target site, OT-4, by SURVEYOR assay (Hsu et al., 2013; Figure 3B, right), suggesting that DN can potentially reduce the likelihood of off-target modifications.

Using deep sequencing to assess modification at five different sgRNA 1 off-target loci (Figure 3A), we observed significant mutagenesis at all sites with wild-type Cas9 + sgRNA 1 (Figure 3C). In contrast, cleavage by Cas9n at 5 off-target sites tested was barely detectable above background sequencing error. Using the ratio of on- to off-target modification levels as a metric of specificity, we found that Cas9n with a pair of sgRNAs was able to achieve >100-fold greater specificity relative to wild-type Cas9 with one of the sgRNAs (Figure 3D). We conducted additional off-target analysis by deep sequencing for two sgRNA pairs (offsets of +16 and +20 bp) targeting the *VEGFA* locus, with similar results (Figure 3E). DN at these off-target loci (Table S5) was able to achieve 200- to >1,500-fold greater specificity than the wild-type Cas9 (Figure 3F and Table S1). Taken together, these results demonstrate that Cas9-mediated double nicking minimizes off-target mutagenesis and is suitable for genome editing with increased specificity.

Double Nicking Facilitates High-Efficiency Homology-Directed Repair, NHEJ-Mediated DNA Insertion, and Genomic Microdeletions

DSBs can stimulate homology-directed repair (HDR) to enable highly precise editing of genomic target sites. To evaluate DN-induced HDR, we targeted the human *EMX1* locus with pairs of sgRNAs offset by −3 and +18 bp (generating 31 and 52 bp 5′ overhangs), respectively, and introduced a single-stranded oligodeoxynucleotide (ssODN) bearing a *Hin*dIII restriction site as the HDR repair template (Figure 4A). Each DN sgRNA pair successfully induced HDR at frequencies higher than those of single-guide Cas9n nickases and comparable to those of wild-type Cas9 (Figure 4B). Furthermore, genome editing in embryonic stem cells or patient-derived induced pluripotent stem cells represents a key opportunity for generating and studying new disease paradigms as well as developing new therapeutics. Because single-nick approaches to inducing HDR in human embryonic stem cells (hESCs) have met with limited success (Hsu et al., 2013), we attempted DN in the HUES62 hES cell line and observed successful HDR (Figure 4C).

To further characterize how offset sgRNA spacing affects the efficiency of HDR, we next tested in HEK 293FT cells a set of sgRNA pairs in which the cleavage site of at least one sgRNA is situated near the site of recombination (overlapping with the HDR ssODN donor template arm). We observed that sgRNA pairs generating 5′ overhangs and having at least one nick occurring within 22 bp of the homology arm are able to induce HDR at levels comparable to those of wild-type Cas9-mediated HDR and significantly greater than those of single Cas9n-sgRNA nicking. In contrast, we did not observe HDR with sgRNA pairs that generated 3′ overhangs or double nicking of the same DNA strand (Figure 4D).

The ability to create defined overhangs could enable precise insertion of donor repair templates containing compatible overhangs via NHEJ-mediated ligation (Maresca et al., 2013). To explore this alternative strategy for transgene insertion, we targeted the *EMX1* locus with Cas9n and an sgRNA pair designed to generate a 43 bp 5′ overhang near the stop codon and supplied a double-stranded oligonucleotide (dsODN) duplex with matching overhangs (Figure 5A). The annealed dsODN insert, containing multiple epitope tags and a restriction site, was successfully integrated into the target (1 out of 37 screened by Sanger sequencing of cloned amplicons). This ligation-based strategy thus illustrates an effective approach for inserting dsODNs encoding short modifications such as protein tags or recombination sites into an endogenous locus.

Additionally, we targeted combinations of sgRNA pairs (four sgRNAs per combination) to the *DYRK1A* locus in HEK 293FT cells to facilitate genomic microdeletions. We generated a set of sgRNAs to mediate 0.5 kb, 1 kb, 2 kb, and 6 kb deletions (Figure 5B and Table S2; sgRNAs 32, 33, and 54–61) and verified successful multiplex nicking-mediated deletion over these ranges via PCR screen of predicted deletion sizes.

Figure 3. Double Nicking Facilitates Efficient Genome Editing in Human Cells

(A) Schematic illustrating Cas9n double nicking (red arrows) the human *EMX1* locus. Five off-target loci with sequence homology to *EMX1* target 1 were selected to screen for Cas9n specificity.

(B) On-target modification rate by Cas9n and a pair of sgRNAs is comparable to those mediated by wild-type Cas9 and single sgRNAs (left). Cas9-sgRNA 1 complexes generate significant off-target mutagenesis, whereas no off-target locus modification is detected with Cas9n (right).

(C) Five off-target loci of sgRNA 1 are examined for indel modifications by deep sequencing of transfected HEK 293FT cells. n = 3; error bars show mean ± SEM.

(D) Specificity comparison of Cas9n with double nicking and wild-type Cas9 with sgRNA alone at the off-target sites. Specificity ratio is calculated as on-target/off-target modification rates. n = 3; error bars show mean ± SEM.

(E and F) Double nicking minimizes off-target modification at two additional human *VEGFA loci* while maintaining high specificity (on/off-target modification ratio). n = 3; error bars show mean ± SEM.

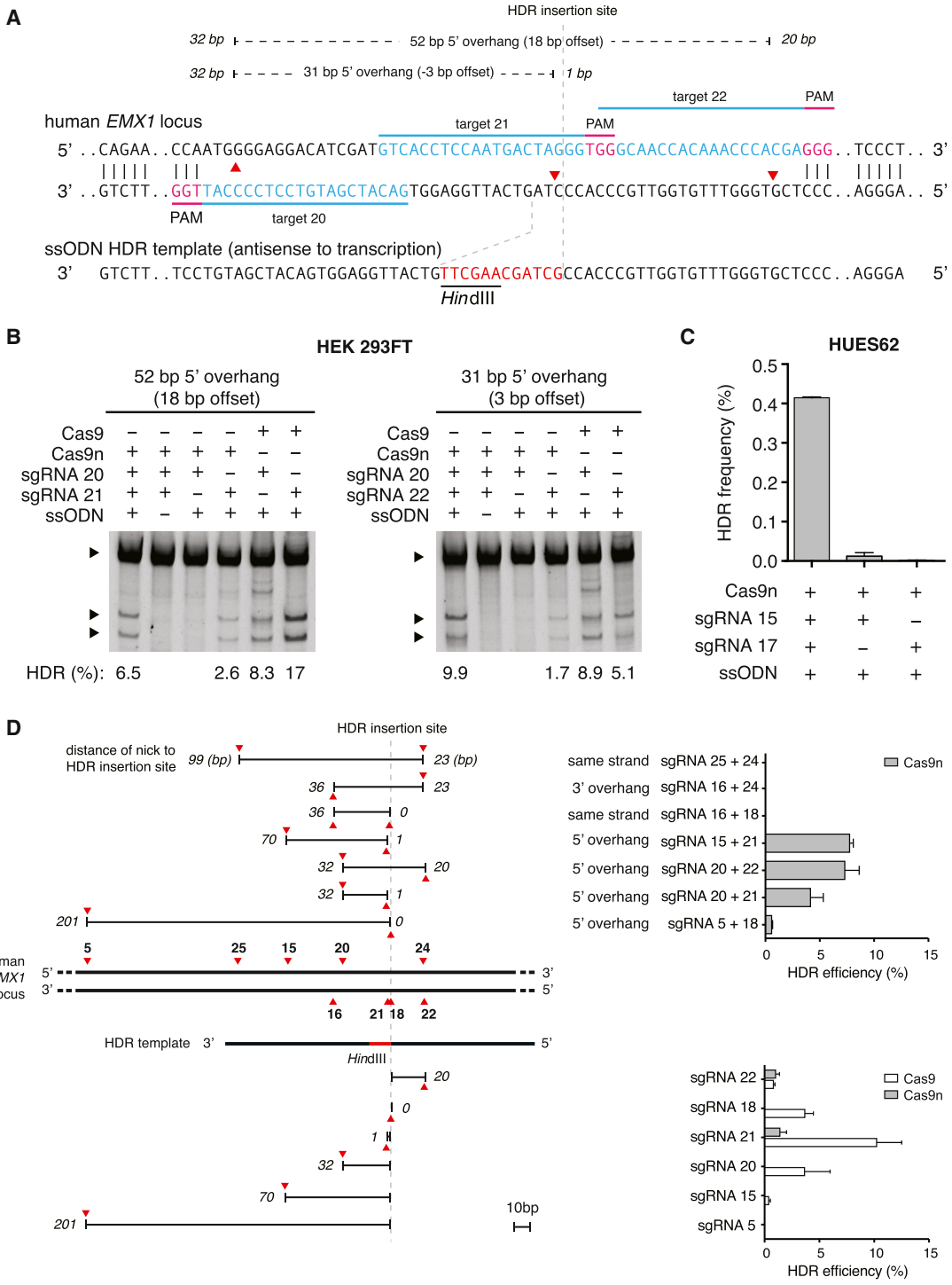

Figure 4. Double Nicking Allows Insertion into the Genome via HDR in Human Cells

(A) Schematic illustrating HDR mediated via a single-stranded oligodeoxynucleotide (ssODN) template at a DSB created by a pair of Cas9n enzymes. A 12 nt sequence (red), including a *Hin*dIII restriction site, is inserted into the *EMX1* locus at the position marked by the gray dashed lines; distances of Cas9n-mediated nicks from the HDR insertion site are indicated on top in italics.

(B) Restriction digest assay gel showing successful insertion of *Hin*dIII cleavage sites by double-nicking-mediated HDR in HEK293FT cells. Top bands are unmodified template; bottom bands are HindIII cleavage product.

(C) Double nicking promotes HDR in the HUES62 human embryonic stem cell line. HDR frequencies are determined by deep sequencing. n = 3; error bars show mean ± SEM.

(legend continued on next page)

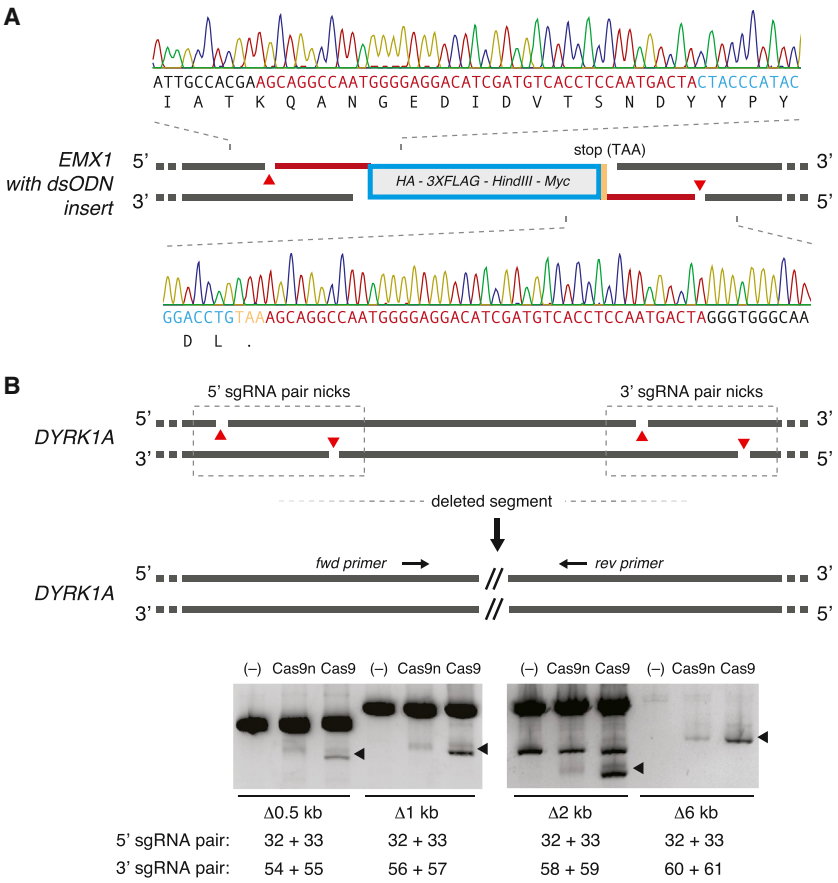

Figure 5. Multiplexed Nicking Facilitates Non-HR-Mediated Gene Integration and Genomic Deletions

(A) Schematic showing insertion of a double-stranded oligodeoxynucleotide (dsODN) donor fragment bearing overhangs complementary to 5′ overhangs created by Cas9 double nicking. The dsODN was designed to remove the native *EMX1* stop codon and contains a HA tag, 3× FLAG tag, *Hin*dIII restriction site, *Myc* epitope tag, and a stop codon in frame, totaling 148 bp. Successful insertion was verified by Sanger sequencing as shown (1 out of 37 clones screened). Amino acid translation of the modified locus is shown below the DNA sequence.

(B) Co-delivery of four sgRNAs with Cas9n generates long-range genomic deletions in the DYRK1A locus (from 0.5 to 6 kb). Deletion was detected using primers (Table S6) spanning the target region.

Double Nicking Enables Efficient Genome Modification in Mouse Zygotes

Recent work demonstrated that co-delivery of wild-type Cas9 mRNA along with multiple sgRNAs can mediate single-step generation of transgenic mice carrying multiple allelic modifications (Wang et al., 2013). Given the ability to achieve genome modification in vivo using several sgRNAs at once, we sought to assess the efficiency of multiple nicking by Cas9n in mouse zygotes. Cytoplasmic coinjection of wild-type Cas9 or Cas9n mRNA and sgRNAs into single-cell mouse zygotes allowed successful targeting of the *Mecp2* locus (Figure 6A). To identify the optimal concentration of Cas9n mRNA and sgRNA for efficient gene targeting, we titrated Cas9 mRNA from 100 to 3 ng/ul while maintaining the sgRNA levels at a 1:20 Cas9:sgRNA molar ratio. All concentrations tested for Cas9 double-nicking-mediated modifications in at least 80% of embryos screened, similar to levels achieved by wild-type Cas9 (Figure 6B). Taken together, these results suggest a number of applications for double-nicking-based genome editing.

DISCUSSION

Given the permanent nature of genomic modifications, specificity is of paramount importance to sensitive applications such as studies aimed at linking specific genetic variants with biological processes or disease phenotypes and gene therapy. Here, we have explored strategies to improve the targeting specificity of Cas9. Although simply extending the guide sequence length of sgRNA failed to improve targeting specificity, combining two appropriately offset sgRNAs with Cas9n effectively generated indels while minimizing unwanted cleavage because individual off-target single-stranded nicks are repaired with high fidelity via base excision repair. Given that significant off-target mutagenesis has been previously reported for Cas9 nucleases in human cells (Fu et al., 2013; Hsu et al., 2013), the DN approach could provide a generalizable solution for rapid and accurate genome editing. The characterization of spacing parameters governing successful Cas9 double-nickase-mediated gene targeting reveals an effective offset window >100 bp long, allowing for a high degree of flexibility in the selection of sgRNA pairs. Previous computational analyses have revealed an average targeting range of every 12 bp for the *Streptococcus pyogenes* Cas9 in the human genome based on the 5′ NGG PAM (Cong et al., 2013), suggesting that appropriate sgRNA pairs should be readily identifiable for most loci within the genome. We have additionally demonstrated DN-mediated indel frequencies comparable to wild-type Cas9 modification at multiple genes and loci in both human and mouse cells, confirming the reproducibility of this strategy for high-precision genome engineering (Table S1).

(D) HDR efficiency depends on the configuration of Cas9 or Cas9n-mediated nicks. HDR is facilitated when a nick occurs near the center of the ssODN homology arm (HDR insertion site), leading to a 5′ resulting overhang. Nicking configurations are annotated with position and strand (red arrows) and length of overhang (black lines) (left). The distance (bp) of each nick from the HDR insertion site is indicated at the end of the black lines in italics, and the positions of the sgRNAs are illustrated in bold on the schematic of the *EMX1* locus. HDR efficiency mediated by double nicking with paired sgRNAs (top) or single sgRNAs with either Cas9 or Cas9n are shown (bottom and Table S2). n = 3; error bars show mean ± SEM.

Please cite this article in press as: Ran et al., Double Nicking by RNA-Guided CRISPR Cas9 for Enhanced Genome Editing Specificity, Cell (2013), http://dx.doi.org/10.1016/j.cell.2013.08.021

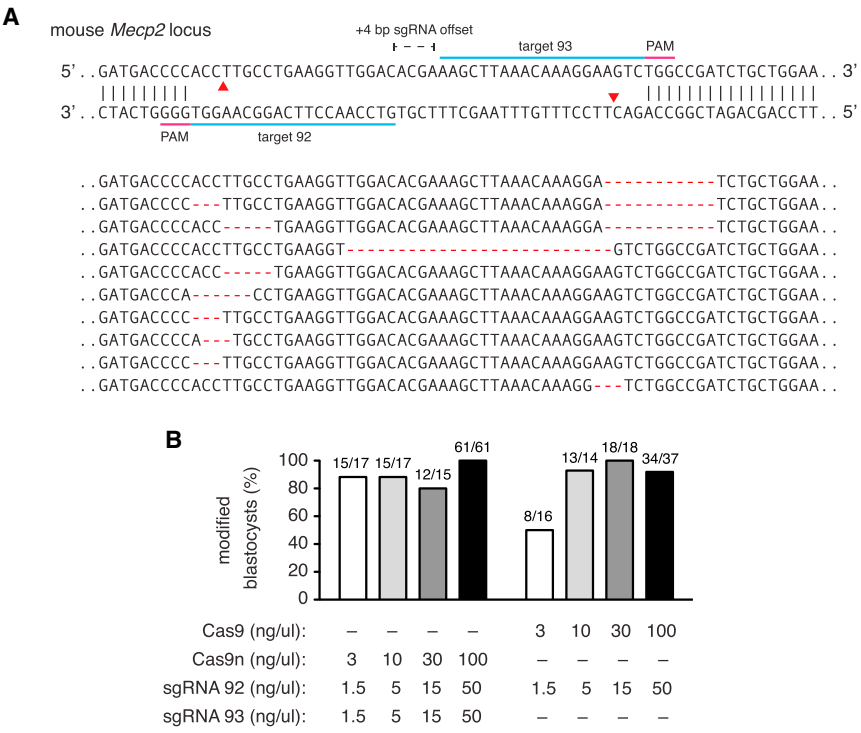

Figure 6. Cas9 Double Nicking Mediates Efficient Indel Formation in Mouse Embryos

(A) Schematic illustrating Cas9n double nicking the mouse *Mecp2* locus. Representative indels are shown for mouse blastocysts coinjected with in-vitro-transcribed Cas9n-encoding mRNA and sgRNA pairs matching targets 92 and 93.

(B) Efficient blastocyst modification is achieved at multiple concentrations of sgRNAs (1.5 to 50 ng/ul) and wild-type Cas9 or Cas9n (3 to 100 ng/ul).

The Cas9 double nicking approach is, in principle, similar to ZFN- and TALEN-based genome editing systems, in which cooperation between two heminuclease domains is required to achieve double-stranded break at the target site. Systematic studies of ZFN and TALEN systems have revealed that the targeting specificity of a given ZFN and TALEN pair can be highly dependent on the nuclease architecture (homo- or heterodimeric nucleases) or target sequence, and in some cases TALENs can be highly specific (Ding et al., 2013). Although the wild-type Cas9 system has been shown to exhibit high levels of off-target mutagenesis, the DN system is a promising solution and brings RNA-guided genome editing to similar specificity levels as ZFNs and TALENs.

Additionally, the ease and efficiency with which Cas9 can be targeted renders the DN system especially attractive. However, DNA targeting using DN will likely face similar off-target challenges as ZFNs and TALENs, in which cooperative nicking at off-target sites might still occur, albeit at a significantly reduced likelihood. Given the extensive characterization of Cas9 specificity and sgRNA mutation analysis (Fu et al., 2013; Hsu et al., 2013), as well as the NHEJ-mediating sgRNA offset range identified in this study, computational approaches may be used to evaluate the likely off-target sites for a given pair of sgRNAs. To facilitate sgRNA pair selection, we developed an online web tool that identifies sgRNA combinations with optimal spacing for double nicking applications (http://www.genome-engineering.org/).

Although Cas9n has been previously shown to facilitate HDR at on-target sites (Cong et al., 2013), its efficiency is substantially lower than that of wild-type Cas9. The double nicking strategy, by comparison, maintains high on-target efficiencies while reducing off-target modifications to background levels. Nevertheless, further characterizations of DN off-target activity, particularly via whole-genome sequencing and targeted deep sequencing of cells or whole organisms generated using the DN approach, are urgently needed to evaluate the utility of Cas9n DN in biotechnological or clinical applications that require ultrahigh-precision genome editing. Additionally, Cas9n has been shown to induce low levels of indels at on-target sites for certain sgRNAs (Mali et al., 2013b), which may result from residual double-strand break activities and may be circumvented by further structure-function studies of Cas9 catalytic activity. Overall, Cas9n-mediated multiplex nicking serves as a customizable platform for highly precise and efficient targeted genome engineering and promises to broaden the range of applications in biotechnology, basic science, and medicine.

EXPERIMENTAL PROCEDURES

Cell Culture and Transfection

Human embryonic kidney (HEK) cell line 293FT (Life Technologies) cell line was maintained in Dulbecco's modified Eagle's medium (DMEM) supplemented with 10% fetal bovine serum (HyClone), 2 mM GlutaMAX (Life Technologies), 100 U/ml penicillin, and 100 μg/ml streptomycin at 37°C with 5% CO_2 incubation.

Cells were seeded onto 24-well plates (Corning) at a density of 120,000 cells/well, 24 hr prior to transfection. Cells were transfected using Lipofectamine 2000 (Life Technologies) at 80%–90% confluency following the manufacturer's recommended protocol. A total of 500 ng Cas9 plasmid and 100 ng of U6-sgRNA PCR product was transfected.

Human embryonic stem cell line HUES62 (Harvard Stem Cell Institute core) was maintained in feeder-free conditions on GelTrex (Life Technologies) in mTesR medium (StemCell Technologies) supplemented with 100 ug/ml Normocin (InvivoGen). HUES62 cells were transfected with Amaxa P3 Primary Cell 4-D Nucleofector Kit (Lonza) following the manufacturer's protocol.

SURVEYOR Nuclease Assay for Genome Modification

HEK 293FT and HUES62 cells were transfected with DNA as described above. Cells were incubated at 37°C for 72 hr posttransfection prior to genomic DNA extraction. Genomic DNA was extracted using the QuickExtract DNA Extraction Solution (Epicenter) following the manufacturer's protocol. In brief, pelleted cells were resuspended in QuickExtract solution and were incubated at 65°C for 15 min, 68°C for 15 min, and 98°C for 10 min.

The genomic region flanking the CRISPR target site for each gene was PCR amplified (Table S3), and products were purified using QiaQuick Spin Column (QIAGEN) following the manufacturer's protocol. 400 ng total of the purified PCR products were mixed with 2 μl 10× Taq DNA Polymerase PCR buffer

(Enzymatics) and ultrapure water to a final volume of 20 μl and were subjected to a reannealing process to enable heteroduplex formation: 95°C for 10 min; 95°C to 85°C ramping at –2°C/s; 85°C to 25°C at – 0.25°C/s; and 25°C hold for 1 min. After reannealing, products were treated with SURVEYOR nuclease and SURVEYOR enhancer S (Transgenomics) following the manufacturer's recommended protocol were and analyzed on 4%–20% Novex TBE polyacrylamide gels (Life Technologies). Gels were stained with SYBR Gold DNA stain (Life Technologies) for 30 min and were imaged with a Gel Doc gel imaging system (Bio-Rad). Quantification was based on relative band intensities. Indel percentage was determined by the formula $100 \times (1 - (1 - (b + c)/(a + b + c))^{1/2})$, wherein a is the integrated intensity of the undigested PCR product and b and c are the integrated intensities of each cleavage product.

Northern Blot Analysis of TracrRNA Expression in Human Cells

Northern blots were performed as previously described (Cong et al., 2013). In brief, RNAs were extracted using the mirPremier microRNA Isolation Kit (Sigma) and were heated to 95°C for 5 min before loading on 8% denaturing polyacrylamide gels (SequaGel, National Diagnostics). Afterward, RNA was transferred to a prehybridized Hybond N+ membrane (GE Healthcare) and was crosslinked with Stratagene UV Crosslinker (Stratagene). Probes were labeled with [γ-32P] ATP (Perkin Elmer) with T4 polynucleotide kinase (New England Biolabs). After washing, membrane was exposed to phosphor screen for 1 hr and scanned with phosphorimager (Typhoon).

Deep Sequencing to Assess Targeting Specificity

HEK293FT cells were plated and transfected as described above 72 hr prior to genomic DNA extraction. The genomic region flanking the CRISPR target site for each gene was amplified (see Table S4 for primer sequences) by a fusion PCR method to attach the Illumina P5 adapters as well as unique sample-specific barcodes to the target. PCR products were purified using EconoSpin 96-well Filter Plates (Epoch Life Sciences) following the manufacturer's recommended protocol.

Barcoded and purified DNA samples were quantified by Qubit 2.0 Fluorometer (Life Technologies) and were pooled in an equimolar ratio. Sequencing libraries were then sequenced with the Illumina MiSeq Personal Sequencer (Life Technologies).

Sequencing Data Analysis, Indel Detection, and Homologous Recombination Detection

MiSeq reads were filtered by requiring an average Phred quality (Q score) of at least 30, as well as perfect sequence matches to barcodes and amplicon forward primers. Reads from on- and off-target loci were analyzed by performing Ratcliff-Obershelp string comparison, as implemented in the Python difflib module, against loci sequences that included 30 nt upstream and downstream of the target site (a total of 80 bp). The resulting edit operations were parsed, and reads were counted as indels if insertion or deletion operations were found. Analyzed target regions were discarded if part of their alignment fell outside of the MiSeq read itself or if more than five bases were uncalled.

Negative controls for each sample provided a gauge for the inclusion or exclusion of indels as putative cutting events. For quantification of homologous recombination, reads were first processed as in the indel detection workflow and were then checked for presence of homologous recombination template CCAGGCTTGG.

Microinjection into Mouse Zygotes

Cas9 mRNA and sgRNA templates were amplified with T7 promoter sequence-conjugated primers. After gel purification, Cas9 and Cas9n were transcribed with mMESSAGE mMACHINE T7 Ultra Kit (Life Technologies). sgRNAs were transcribed with MEGAshortscript T7 Kit (Life Technologies). RNAs were purified by MEGAclear Kit (Life Technologies) and frozen at –80°C.

MII-stage oocytes were collected from 8-week-old superovulated BDF1 females by injecting 7.5 I.U. of PMSG (Harbor, UCLA) and hCG (Millipore). They were transferred into HTF medium supplemented with 10 mg/ml bovine serum albumin (BSA; Sigma-Aldrich) and were inseminated with capacitated sperm obtained from the caudal epididymides of adult C57BL/6 male mice. Six hours after fertilization, zygotes were injected with mRNAs and sgRNAs in M2 media (Millipore) using a Piezo impact-driven micromanipulator (Prime Tech Ltd., Ibaraki, Japan). The concentrations of Cas9 and Cas9n mRNAs and sgRNAs are described in the text and Figure 6B. After microinjection, zygotes were cultured in KSOM (Millipore) in a humidified atmosphere of 5% CO_2 and 95% air at 37°C.

Genome Extraction from Blastocyst Embryos

Following in vitro culture of embryos for 6 days, the expanded blastocysts were washed with 0.01% BSA in PBS and were individually collected into 0.2 ml tubes. Five microliters of genome extraction solution (50 mM Tris-HCl [pH 8.0], 0.5% Triton X-100, and 1 mg/ml Proteinase K) were added and the samples were incubated in 65°C for 3 hr followed by 95°C for 10 min. Samples were then amplified for targeted deep sequencing as described above.

SUPPLEMENTAL INFORMATION

Supplemental Information includes Extended Experimental Procedures and six tables and can be found with this article online at http://dx.doi.org/10.1016/j.cell.2013.08.021.

ACKNOWLEDGMENTS

We thank Joshua Weinstein and Yinqing Li for statistical consultation, Xuebing Wu and Phillip Sharp for assistance with northern blotting experiments, Su Vora for help with the manuscript, and the entire Zhang lab for their support and advice. P.D.H. is a James Mills Pierce Fellow. C.-Y.L. is supported by T32GM007753 from the National Institute of General Medical Sciences. D.A.S. is an NSF predoctoral fellow. A.I. and S.M. are research fellows for Research Abroad of the Japan Society for the Promotion of Science. Y.Z. is supported by NIH grants GM68804 and U01DK089565 and is an Investigator of the Howard Hughes Medical Institute. F.Z. is supported by an NIH Director's Pioneer Award (1DP1-MH100706), a NIH Transformative R01 grant (1R01-DK097768), the Keck, McKnight, Damon Runyon, Searle Scholars, Klingenstein, Vallee, and Simons Foundations, Bob Metcalfe, and Jane Pauley.

Received: July 25, 2013
Revised: August 13, 2013
Accepted: August 14, 2013
Published: August 29, 2013

REFERENCES

Boch, J., Scholze, H., Schornack, S., Landgraf, A., Hahn, S., Kay, S., Lahaye, T., Nickstadt, A., and Bonas, U. (2009). Breaking the code of DNA binding specificity of TAL-type III effectors. Science *326*, 1509–1512.

Carlson, D.F., Tan, W.F., Lillico, S.G., Stverakova, D., Proudfoot, C., Christian, M., Voytas, D.F., Long, C.R., Whitelaw, C.B.A., and Fahrenkrug, S.C. (2012). Efficient TALEN-mediated gene knockout in livestock. Proc. Natl. Acad. Sci. USA *109*, 17382–17387.

Chang, N., Sun, C., Gao, L., Zhu, D., Xu, X., Zhu, X., Xiong, J.W., and Xi, J.J. (2013). Genome editing with RNA-guided Cas9 nuclease in zebrafish embryos. Cell Res. *23*, 465–472.

Cho, S.W., Kim, S., Kim, J.M., and Kim, J.S. (2013). Targeted genome engineering in human cells with the Cas9 RNA-guided endonuclease. Nat. Biotechnol. *31*, 230–232.

Christian, M., Cermak, T., Doyle, E.L., Schmidt, C., Zhang, F., Hummel, A., Bogdanove, A.J., and Voytas, D.F. (2010). Targeting DNA double-strand breaks with TAL effector nucleases. Genetics *186*, 757–761.

Cong, L., Ran, F.A., Cox, D., Lin, S., Barretto, R., Habib, N., Hsu, P.D., Wu, X., Jiang, W., Marraffini, L.A., and Zhang, F. (2013). Multiplex genome engineering using CRISPR/Cas systems. Science *339*, 819–823.

Deltcheva, E., Chylinski, K., Sharma, C.M., Gonzales, K., Chao, Y., Pirzada, Z.A., Eckert, M.R., Vogel, J., and Charpentier, E. (2011). CRISPR RNA maturation by trans-encoded small RNA and host factor RNase III. Nature *471*, 602–607.

Deveau, H., Garneau, J.E., and Moineau, S. (2010). CRISPR/Cas system and its role in phage-bacteria interactions. Annu. Rev. Microbiol. *64*, 475–493.

Dianov, G.L., and Hübscher, U. (2013). Mammalian base excision repair: the forgotten archangel. Nucleic Acids Res. *41*, 3483–3490.

Ding, Q., Lee, Y.K., Schaefer, E.A., Peters, D.T., Veres, A., Kim, K., Kuperwasser, N., Motola, D.L., Meissner, T.B., Hendriks, W.T., et al. (2013). A TALEN genome-editing system for generating human stem cell-based disease models. Cell Stem Cell *12*, 238–251.

Friedland, A.E., Tzur, Y.B., Esvelt, K.M., Colaiácovo, M.P., Church, G.M., and Calarco, J.A. (2013). Heritable genome editing in C. elegans via a CRISPR-Cas9 system. Nat. Methods *10*, 741–743.

Fu, Y., Foden, J.A., Khayter, C., Maeder, M.L., Reyon, D., Joung, J.K., and Sander, J.D. (2013). High-frequency off-target mutagenesis induced by CRISPR-Cas nucleases in human cells. Nat. Biotechnol. Published online June 23, 2013. http://dx.doi.org/10.1038/nbt.2623.

Gasiunas, G., Barrangou, R., Horvath, P., and Siksnys, V. (2012). Cas9-crRNA ribonucleoprotein complex mediates specific DNA cleavage for adaptive immunity in bacteria. Proc. Natl. Acad. Sci. USA *109*, E2579–E2586.

Geurts, A.M., Cost, G.J., Freyvert, Y., Zeitler, B., Miller, J.C., Choi, V.M., Jenkins, S.S., Wood, A., Cui, X.X., Meng, X.D., et al. (2009). Knockout rats via embryo microinjection of zinc-finger nucleases. Science *325*, 433–433.

Gratz, S.J., Cummings, A.M., Nguyen, J.N., Hamm, D.C., Donohue, L.K., Harrison, M.M., Wildonger, J., and O'Connor-Giles, K.M. (2013). Genome engineering of Drosophila with the CRISPR RNA-guided Cas9 nuclease. Genetics *194*, 1029–1035.

Horvath, P., and Barrangou, R. (2010). CRISPR/Cas, the immune system of bacteria and archaea. Science *327*, 167–170.

Hsu, P.D., and Zhang, F. (2012). Dissecting neural function using targeted genome engineering technologies. ACS Chem. Neurosci. *3*, 603–610.

Hsu, P.D., Scott, D.A., Weinstein, J.A., Ran, F.A., Konermann, S., Agarwala, V., Li, Y., Fine, E.J., Wu, X., Shalem, O., et al. (2013). DNA targeting specificity of RNA-guided Cas9 nucleases. Nat. Biotechnol. Published online July 21, 2013. http://dx.doi.org/10.1038/nbt.2647.

Jiang, W., Bikard, D., Cox, D., Zhang, F., and Marraffini, L.A. (2013). RNA-guided editing of bacterial genomes using CRISPR-Cas systems. Nat. Biotechnol. *31*, 233–239.

Jinek, M., Chylinski, K., Fonfara, I., Hauer, M., Doudna, J.A., and Charpentier, E. (2012). A programmable dual-RNA-guided DNA endonuclease in adaptive bacterial immunity. Science *337*, 816–821.

Jinek, M., East, A., Cheng, A., Lin, S., Ma, E., and Doudna, J. (2013). RNA-programmed genome editing in human cells. eLife *2*, e00471.

Mali, P., Aach, J., Stranges, P.B., Esvelt, K.M., Moosburner, M., Kosuri, S., Yang, L., and Church, G.M. (2013a). CAS9 transcriptional activators for target specificity screening and paired nickases for cooperative genome engineering. Nat. Biotechnol. Published online August 1, 2013. http://dx.doi.org/10.1038/nbt.2675.

Mali, P., Yang, L., Esvelt, K.M., Aach, J., Guell, M., DiCarlo, J.E., Norville, J.E., and Church, G.M. (2013b). RNA-guided human genome engineering via Cas9. Science *339*, 823–826.

Maresca, M., Lin, V.G., Guo, N., and Yang, Y. (2013). Obligate ligation-gated recombination (ObLiGaRe): custom-designed nuclease-mediated targeted integration through nonhomologous end joining. Genome Res. *23*, 539–546.

Miller, J.C., Holmes, M.C., Wang, J., Guschin, D.Y., Lee, Y.L., Rupniewski, I., Beausejour, C.M., Waite, A.J., Wang, N.S., Kim, K.A., et al. (2007). An improved zinc-finger nuclease architecture for highly specific genome editing. Nat. Biotechnol. *25*, 778–785.

Miller, J.C., Tan, S., Qiao, G., Barlow, K.A., Wang, J., Xia, D.F., Meng, X., Paschon, D.E., Leung, E., Hinkley, S.J., et al. (2011). A TALE nuclease architecture for efficient genome editing. Nat. Biotechnol. *29*, 143–148.

Moscou, M.J., and Bogdanove, A.J. (2009). A simple cipher governs DNA recognition by TAL effectors. Science *326*, 1501.

Pattanayak, V., Lin, S., Guilinger, J.P., Ma, E., Doudna, J.A., and Liu, D.R. (2013). High-throughput profiling of off-target DNA cleavage reveals RNA-programmed Cas9 nuclease specificity. Nat. Biotechnol. Published online August 11, 2013. http://dx.doi.org/10.1038/nbt.2673.

Perez, E.E., Wang, J.B., Miller, J.C., Jouvenot, Y., Kim, K.A., Liu, O., Wang, N., Lee, G., Bartsevich, V.V., Lee, Y.L., et al. (2008). Establishment of HIV-1 resistance in CD4+ T cells by genome editing using zinc-finger nucleases. Nat. Biotechnol. *26*, 808–816.

Porteus, M.H., and Baltimore, D. (2003). Chimeric nucleases stimulate gene targeting in human cells. Science *300*, 763.

Reyon, D., Tsai, S.Q., Khayter, C., Foden, J.A., Sander, J.D., and Joung, J.K. (2012). FLASH assembly of TALENs for high-throughput genome editing. Nat. Biotechnol. *30*, 460–465.

Sander, J.D., Dahlborg, E.J., Goodwin, M.J., Cade, L., Zhang, F., Cifuentes, D., Curtin, S.J., Blackburn, J.S., Thibodeau-Beganny, S., Qi, Y., et al. (2011). Selection-free zinc-finger-nuclease engineering by context-dependent assembly (CoDA). Nat. Methods *8*, 67–69.

Sanjana, N.E., Cong, L., Zhou, Y., Cunniff, M.M., Feng, G., and Zhang, F. (2012). A transcription activator-like effector toolbox for genome engineering. Nat. Protoc. *7*, 171–192.

Soldner, F., Laganiere, J., Cheng, A.W., Hockemeyer, D., Gao, Q., Alagappan, R., Khurana, V., Golbe, L.I., Myers, R.H., Lindquist, S., et al. (2011). Generation of isogenic pluripotent stem cells differing exclusively at two early onset Parkinson point mutations. Cell *146*, 318–331.

Takasu, Y., Kobayashi, I., Beumer, K., Uchino, K., Sezutsu, H., Sajwan, S., Carroll, D., Tamura, T., and Zurovec, M. (2010). Targeted mutagenesis in the silkworm Bombyx mori using zinc finger nuclease mRNA injection. Insect Biochem. Mol. Biol. *40*, 759–765.

Urnov, F.D., Rebar, E.J., Holmes, M.C., Zhang, H.S., and Gregory, P.D. (2010). Genome editing with engineered zinc finger nucleases. Nat. Rev. Genet. *11*, 636–646.

Wang, H., Yang, H., Shivalila, C.S., Dawlaty, M.M., Cheng, A.W., Zhang, F., and Jaenisch, R. (2013). One-step generation of mice carrying mutations in multiple genes by CRISPR/Cas-mediated genome engineering. Cell *153*, 910–918.

Watanabe, T., Ochiai, H., Sakuma, T., Horch, H.W., Hamaguchi, N., Nakamura, T., Bando, T., Ohuchi, H., Yamamoto, T., Noji, S., et al. (2012). Non-transgenic genome modifications in a hemimetabolous insect using zinc-finger and TAL effector nucleases. Nat. Commun. *3*. Published online August 21, 2012. http://dx.doi.org/10.1038/ncomms2020.

Wood, A.J., Lo, T.W., Zeitler, B., Pickle, C.S., Ralston, E.J., Lee, A.H., Amora, R., Miller, J.C., Leung, E., Meng, X., et al. (2011). Targeted genome editing across species using ZFNs and TALENs. Science *333*, 307.

Zhang, F., Cong, L., Lodato, S., Kosuri, S., Church, G.M., and Arlotta, P. (2011). Efficient construction of sequence-specific TAL effectors for modulating mammalian transcription. Nat. Biotechnol. *29*, 149–153.